# Noise-Tolerant Fixed-Time Leader-Follower Consensus for Multi-Agent Systems via Fuzzy-Neural-Network Controller Design

Jianhua Dai, Ping Tan, Lin Xiao, Zidong Wang, *Fellow, IEEE*, Yongjun He, and Qiuyue Zuo

***Abstract*—The leader-follower consensus control problem in multi-agent systems (MASs) is critical and has received significant attention. However, the simultaneous achievement of fixed-time stability and robustness is often challenging in MASs due to their inherent complexity and uncertainty. This paper proposes a noise-tolerant fixed-time fuzzy-neural-network controller (NF-FNNC) to realize the leader-follower consensus of MASs by utilizing the adaptability of the Takagi-Sugeno fuzzy logic system (TSFLS). Specifically, the introduction of an integral error term makes the NF-FNNC have powerful noise tolerance, and a fuzzy gain parameter generated by TSFLS makes the NF-FNNC have fuzzy adaptiveness. In addition, a new partition-sign-by-power activation function is developed to ensure fixed-time stability of the NF-FNNC. Theoretical analysis and comparative simulations confirm the superb swift stability and excellent noise tolerance of the NF-FNNC for achieving the leader-follower consensus of MASs, as compared with existing controllers.**

***Index Terms*—Fuzzy neural networks, Takagi-Sugeno fuzzy logic system, multi-agent systems, leader-follower consensus, noise tolerance.**

## I. Introduction

Cooperative control of multi-agent systems (MASs) has been recognized as increasingly important for accomplishing complex tasks [1]–[3]. As the cornerstone of cooperative control, consensus has been applied successfully in various domains such as multi-robot systems [4], mobile sensor networks [5], and unmanned aerial vehicles [6]. In general, consensus in MASs is categorized into leader-follower consensus and leaderless consensus, which are characterized by agents sharing information only with their neighbors, while no global information or centralized processing system are available [7]. Therefore, an effective consensus controller should be designed to allow a collective of agents to reach a harmonious state based on limited information.

So far, consensus control problems for MASs have attracted considerable research interest, and numerous control methods have been proposed. For instance, a distributed dynamic event-triggered strategy has been introduced in [8] to address both leaderless consensus and leader-follower consensus in general linear MASs. In [9], an adaptive asynchronous strategy has been put forward for the consensus problem of uncertain triangular nonlinear MASs. In [10], a novel distributed gradient neural network has been suggested to tackle prevalent consensus challenges in MASs. On the other hand, in modern consensus research, the pursuit of robustness can sometimes lead to the adoption of more cautious control strategies, which might inadvertently affect fixed-time stability [11]. As a result, the simultaneous achievement of fixed-time stability and robustness often becomes challenging.

The recurrent neural network (RNN) has firmly established itself in the realm of control, with several modified neural networks stemming from RNN being extensively studied [12], [13]. Among others, the Zeroing Neural Network (ZNN) [14] stands out for its efficacy in tackling real-time challenges. Compared to traditional RNNs, the ZNN effectively curtails the lag error that accumulates over time. By now, various modified ZNN models have been leveraged for control tasks including acoustic source localization [15], synchronization of chaotic systems [16], and robot trajectory tracking [17].

Given the remarkable capabilities demonstrated by ZNN in real-time control scenarios, it is imperative to craft a new leader-follower consensus control protocol that harnesses the ZNN methodology, where the convergence rate remains a crucial metric for neural network techniques. In the existing literature, certain advanced ZNN methods have exhibited both exponential convergence [14] and finite-time convergence [18], [19]. Nonetheless, exponential convergence does not allow for predicting the convergence duration, while the convergence time in finite-time convergence can be affected by the initial state. Hence, fixed-time convergence presents a more practical advantage [16].

Traditional ZNN models are notably sensitive to noise, a challenge considering noise is inescapable in practical control applications. As a result, much research effort has been devoted to the performance enhancement of ZNN in the presence of noise perturbations, and the most common strategy for instilling noise-tolerance in neural network models is the integration of terms that accumulate historical errors. For example, an advanced ZNN model, termed the NZNN model, has been presented in [18] that boasts significant noise resilience and attains finite-time convergence when addressing certain nonlinear optimization problems. Impressively, the NZNN model can pinpoint the optimal solution despite the presence of various external noises. Furthermore, in [20], a ZNN model with both finite-time convergence and robustness has been devised to

This work was supported in part by the National Natural Science Foundation of China under Grant 61866013.

J. Dai, P. Tan, L. Xiao, Y. He, and Q. Zuo are with Hunan Provincial Key Laboratory of Intelligent Computing and Language Information Processing, Hunan Normal University, and also with MOE-LCSM, Hunan Normal University, Changsha 410081, China. (e-mail: xiaolin860728@163.com).

Z. Wang is with Department of Computer Science, Brunel University London, Uxbridge, Middlesex, UB8 3PH, United Kingdom (e-mail: zidong.wang@brunel.ac.uk).

tackle the Moore-Penrose inversion of dynamic matrices, and such a ZNN model has been applied to the real-time path-following problem of redundant manipulators.

Very recently, a closed-loop model has been unveiled in [21] for continuous motion estimation by integrating the noise-resilient ZNN method with the long short-term memory network. This model displays a marked superiority in prediction accuracy and noise attenuation as compared to existing solutions. Moreover, it is of practical significance to design a noise-resistant controller with formidable disturbance rejection capabilities so as to amplify a controller's adaptability and flexibility. As shown in [16], the noise-resistant controller design can also bolster the system's safety and stability, and these attributes underscore the profound importance and relevance of noise-resistant controllers in real-world applications.

As evidenced in [19], [22], appropriate variable gain parameters can substantially elevate the efficacy of the ZNN approach, thereby outperforming fixed gain parameters. Yet, variable gain parameters might encounter the parameter explosion issue over time. Conversely, selecting fixed gain parameters often proves challenging particularly in real-time problem computations [23]. On the other hand, the fuzzy logic system (FLS) is renowned for its prowess in addressing complex nonlinear challenges and has consistently demonstrated valuable insights into dynamic systems [24]. The FLS can operate even with incomplete system data and is recognized for its exceptional fault tolerance and robustness [25]. Employing the FLS to generate fuzzy gain parameters for neural networks offers an alternative to both fixed and variable gain parameters, effectively sidestepping their inherent drawbacks.

Up to now, several FLS-based modified neural network models have been explored. For example, the interplay between FLSs and the ZNN method has been examined in [26]. In [27], two intricate fuzzy neural network models have been introduced by utilizing adaptive design parameters over their fixed or time-varying counterparts. Moreover, in [28], an intelligent fuzzy robust neural network model has been proposed that combines the ZNN methodology with FLS according to the time-varying Stein matrix equations. Nonetheless, most existing studies have predominantly employed the Madani FLS. In contrast, the Takagi-Sugeno FLS (TSFLS) offers a streamlined approach for minimizing computational complexity [29], and such computational efficiency positions the TSFLS as a preferable option for real-time scenarios

Pertaining to the above discussions, in this paper, we investigate a noise-tolerant fixed-time fuzzy-neural-network controller (NF-FNNC) integrated with the TSFLS to address the leader-follower consensus problem in MASs. Specifically, the incorporation of an error integral term in the NF-FNNC's design endows it with robust noise tolerance. Simultaneously, by leveraging a fuzzy gain parameter produced by the TSFLS, the NF-FNNC attains adaptive control performance. Furthermore, we introduce and implement a novel partition-sign-by-power activation function (PSBPAF) within the NF-FNNC so as to ensure that the MAS achieves consensus within a predetermined time frame. Theoretical analysis underscores the fixed-time stability and resilience of the NF-FNNC, and also stipulates a less conservative upper bound for the stabilization time of the NF-FNNC. Numerical simulations conducted across diverse settings further showcase the NF-FNNC's superior convergence rate and satisfactory noise resistance when contrasted with other control methodologies.

The key contributions of this study can be distilled into the following four aspects.

1) A noise-tolerant fixed-time fuzzy-neural-network controller is developed that is tailored for the leader-follower consensus in MASs, which marks the inaugural application of the ZNN method to address leader-follower consensus challenges.
2) Leveraging the proposed PSBPAF, the NF-FNNC achieves quicker stabilization within a fixed-time frame than those by alternative methods.
3) In response to the monitored system state, we employ the TSFLS to dynamically adjust the gain parameter of the NF-FNNC, thereby bolstering its adaptive robustness.
4) A comprehensive theoretical analysis confirms the fixed-time stability and noise resilience of systems deploying our proposed NF-FNNC, where numerical simulations further corroborate the superior efficacy of our method in handling the leader-follower consensus within MASs.

The structure of this paper unfolds as follows. Section II furnishes essential background information. In Section III, we define the research objectives and elucidate the design process behind NF-FNNC. Section IV presents several theorems that evaluate the efficacy of NF-FNNC in both noise-free and noisy conditions. Numerical simulation outcomes are shared in Section V. Finally, the paper's conclusions are drawn in Section VI.

## II. Preliminaries

In this section, we aim to provide basic concepts of graph theory and detail the design methodology of the TSFLS for improved comprehension. Furthermore, we will present several lemmas to reinforce the subsequent proof framework.

### A. Graph Theory

The directed graph $\mathcal{G} = \{\mathcal{V}, \mathcal{E}, \mathcal{A}\}$ is utilized to represent the topology structure of the MAS consisting of $n$ agents. Here, $\mathcal{V} = \{v_1, v_2, ..., v_n\}$ denotes the set of nodes, $\mathcal{E} \subseteq \{(v_i, v_j)|v_i, v_j \in \mathcal{V}$ and $i \neq j\}$ represents the set of edges connecting the nodes, and $\mathcal{A} = [a_{ij}] \in \mathbb{R}^{n\times n}$ is the adjacency matrix defined as

$$a_{ij} = \begin{cases} 1, \text{ if } j \in \mathcal{N}_i, \\ 0, \text{ else}, \end{cases}$$

where $\mathcal{N}_i$ represents the set of neighbor nodes to node $i$. The in-degree matrix is defined as $\mathcal{D} = \mathrm{diag}\{d_1, d_2, ..., d_n\}$ with $d_i = \sum_{j\neq i} a_{ij}$. The Laplace matrix $\mathcal{L}$ is defined as $\mathcal{L} = \mathcal{D} - \mathcal{A}$.

For an MAS with one leader and $n$ followers, information is exchanged among the $n+1$ agents, and the topology is denoted as $\hat{\mathcal{G}} = \{\mathcal{V}, \mathcal{E}, \mathcal{A}, \mathcal{A}'\}$, which has an additional leader agent compared to $\mathcal{G}$. In particular, $\mathcal{A}' = \mathrm{diag}\{\hat{a}_1, \hat{a}_2, ..., \hat{a}_n\}$ indicates the leader adjacency matrix, in which $\hat{a}_i = 1$ if there exists communication from the leader to agent $i$, and $\hat{a}_i = 0$ otherwise.

### B. Takagi-Sugeno Fuzzy Logic System

The proposed NF-FNNC utilizes the output of TSFLS as the fuzzy gain parameter to achieve adaptive control. In particular, system error norm $\varpi_1 = \|\boldsymbol{e}(t)\|$ and error derivative norm $\varpi_2 = -\|\dot{\boldsymbol{e}}(t)\|$ are employed as the input of TSFLS to reflect the system state, and the output $\eta$ is generated by the preset fuzzy logic scheme. Typically, the design process of TSFLS usually consists of three steps: fuzzification, fuzzy reasoning, and defuzzification [29].

*Fuzzification*: In this step, the input $\varpi_1$ and $\varpi_2$ should be mapped to the corresponding fuzzy value based on membership functions. In this paper, the Gaussian membership function $M_g(\cdot)$ is employed to fuzzify $\varpi_1$, while the triangular membership function $M_t(\cdot)$ is utilized to fuzzify $\varpi_2$. The expressions of two membership functions are given as follows [29]:

- Gaussian membership function:

$$M_g(\tau) = \exp\left(-\frac{(\tau - c)^2}{2\sigma^2}\right), \tag{1}$$

where $c$ and $\sigma$ are positive constants.

- Triangular membership function:

$$M_t(\tau) = \begin{cases} 0, & \tau \leqslant a_1, \\ \frac{\tau - a_1}{a_2 - a_1}, & a_1 < \tau \leqslant a_2, \\ \frac{a_3 - \tau}{a_3 - a_2}, & a_2 < \tau \leqslant a_3, \\ 0, & \tau \geqslant a_3, \end{cases} \tag{2}$$

where $a_1, a_2$, and $a_3$ are constants satisfying $a_1 < a_2 < a_3$.

*Fuzzy reasoning*: Fuzzy rules are known to play a crucial role in fuzzy reasoning. In this paper, the following if-then rules are provided as the fuzzy rule set $\mathcal{R}$ of the TSFLS.
$\mathcal{R}_1$: if $\varpi_1 =$ PL and $\varpi_2 =$ NL, then $o_1 = 4\varpi_1 - 3.5\varpi_2 + 8$;
$\mathcal{R}_2$: if $\varpi_1 =$ PL and $\varpi_2 =$ NM, then $o_2 = 4\varpi_1 - 2.5\varpi_2 + 6$;
$\mathcal{R}_3$: if $\varpi_1 =$ PL and $\varpi_2 =$ NS, then $o_3 = 4\varpi_1 - 1.5\varpi_2 + 4$;
$\mathcal{R}_4$: if $\varpi_1 =$ PL and $\varpi_2 =$ AZ, then $o_4 = 4\varpi_1 - 0.5\varpi_2 + 2$;
$\mathcal{R}_5$: if $\varpi_1 =$ PM and $\varpi_2 =$ NL, then $o_5 = 2\varpi_1 - 4\varpi_2 + 2$;
$\mathcal{R}_6$: if $\varpi_1 =$ PM and $\varpi_2 =$ NM, then $o_6 = 2\varpi_1 - 3\varpi_2 + 4$;
$\mathcal{R}_7$: if $\varpi_1 =$ PM and $\varpi_2 =$ NS, then $o_7 = 2\varpi_1 - 2\varpi_2 + 6$;
$\mathcal{R}_8$: if $\varpi_1 =$ PM and $\varpi_2 =$ AZ, then $o_8 = 2\varpi_1 - \varpi_2 + 8$;
$\mathcal{R}_9$: if $\varpi_1 =$ PS and $\varpi_2 =$ NL, then $o_9 = -4\varpi_2 + 5$;
$\mathcal{R}_{10}$: if $\varpi_1 =$ PS and $\varpi_2 \neq$ NL, then $o_{10} = 10$
where the fuzzy subset PL, PM, and PS denote positive large, positive medium and positive small, respectively; the fuzzy subset NL, NM, NS, and AZ represent negative large, negative medium, negative small, and almost zero, respectively.

In Fig. 1(a), based on the expression of Gaussian membership function (1), the fuzzy subset PS is acquired when $\sigma = 2$ and $c = 0$ in (1); the PM is obtained when $\sigma = 2$ and $c = 4$; and when $\sigma = 2$ and $c = 8$, the PL is acquired. Similarly, in Fig. 1(b), based on the expression of the Triangular membership function (2), the fuzzy subset NM is obtained when $a_1 = -12$, $a_2 = -8$, and $a_3 = -4$.

The product method in [29] is employed to calculate the weight of each rule, and the weight of $\mathcal{R}_i$ can be described as

$$w_i = M_g(\varpi_1) M_t(\varpi_2),\ i = 1, 2, ..., 10,$$

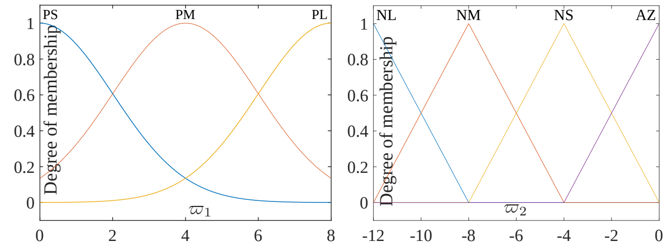

(a) Gaussian (b) Triangular

Fig. 1. Membership functions of the TSFLS.

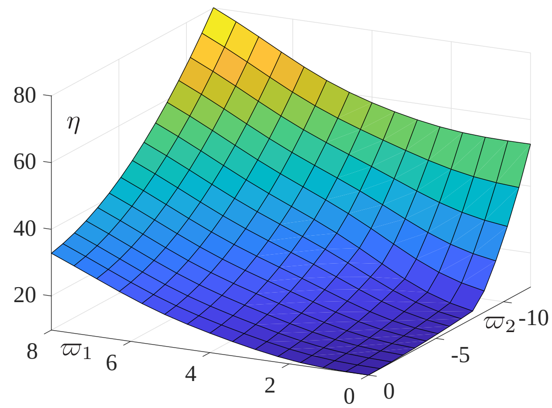

Fig. 2. Surface of the TSFLS.

where $M_g(\varpi_1)$ and $M_t(\varpi_2)$ indicate the membership degree of $\varpi_1$ and $\varpi_2$ in the corresponding rule, respectively.

*Defuzzification*: The defuzzification method, called Weighted Average (Wtaver) [30], is exploited to obtain a precise output $\eta$ of the TSFLS, where $\eta$ can be expressed as

$$\eta = \frac{\sum_{i=1}^{10} w_i o_i}{\sum_{i=1}^{n} w_i}. \tag{3}$$

*Remark 1:* In Fig. 2, the inputs for the TSFLS are represented as $\varpi_1 = \|\boldsymbol{e}(t)\|$ and $\varpi_2 = -\|\dot{\boldsymbol{e}}(t)\|$, while the output, denoted as $\eta$, signifies the fuzzy gain parameter used in the proposed NF-FNNC. This visualization indicates that when both $\varpi_1$ and $\varpi_2$ are small, the resulting $\eta$ is also small; conversely, as $\varpi_1$ and $\varpi_2$ increase, so does the fuzzy gain parameter $\eta$. Notably, the control methodology of the TSFLS is aptly tailored to produce gain parameters for ZNN models, thereby ensuring adaptability. This circumvents issues like parameter explosion or challenges associated with determining the optimal values of existing gain parameters [28].

### C. Lemmas about Stability

*Lemma 1 ( [31]):* The following nonlinear system

$$\dot{\boldsymbol{\delta}}(t) = f(t, \boldsymbol{\delta}(t)), \quad \boldsymbol{\delta}(0) = \boldsymbol{\delta}_0, \tag{4}$$

where $\dot{\boldsymbol{\delta}}(t)$ denotes the time derivative of $\boldsymbol{\delta}(t)$ and $f : \mathbb{D} \to \mathbb{R}^n$ represents a nonlinear function, has an equilibrium point at the origin. Furthermore, if there exist a positive definite function $V(\boldsymbol{\delta}(t)) : \mathbb{D} \to \mathbb{R}$ and real numbers $l, s > 0$, $p > 1$ satisfying

$$\dot{V}(\boldsymbol{\delta}(t)) \leqslant -lV^p(\boldsymbol{\delta}(t)) - sV(\boldsymbol{\delta}(t)), \quad \forall \boldsymbol{\delta}(t) \in \mathbb{U}$$

where $\dot{V}(\boldsymbol{\delta}(t))$ denotes the time derivative of $V(\boldsymbol{\delta}(t))$, then there exists a time $T_1$ such that $V(\boldsymbol{\delta}(T_1)) = 1$ and

$$T_1 \leqslant \frac{\ln\left(1+\frac{s(1-V^{1-p}(\boldsymbol{\delta}_0))}{sV^{1-p}(\boldsymbol{\delta}_0)+l}\right)}{s(p-1)}$$

when $V(\boldsymbol{\delta}_0) \geqslant 1$.

*Lemma 2 ( [32]):* For a system $\dot{\boldsymbol{\delta}}(t) = f(t, \boldsymbol{\delta}(t))$ identical to the one in *Lemma* 1, if there exist a positive definite function $V(\boldsymbol{\delta}(t)) : \mathbb{D} \to \mathbb{R}$ and real numbers $r, s > 0$, $0 < q < 1$ such that

$$\dot{V}(\boldsymbol{\delta}(t)) \leqslant -rV^q(\boldsymbol{\delta}(t)) - sV(\boldsymbol{\delta}(t)), \quad \forall \boldsymbol{\delta}(t) \in \mathbb{U}$$

where $\dot{V}(\boldsymbol{\delta}(t))$ denotes the time derivative of $V(\boldsymbol{\delta}(t))$, then the stabilization time $T(\boldsymbol{\delta}_0)$ satisfies

$$T(\boldsymbol{\delta}_0) \leqslant \frac{\ln(1+\frac{s}{r}V^{1-q}(\boldsymbol{\delta}_0))}{s(1-q)}, \ \boldsymbol{\delta}_0 \in \mathbb{U}.$$

## III. Problem Formulation and Controller Design

In this section, we will formulate the specific problem addressed in this paper and detail the design methodology behind the NF-FNNC. Furthermore, we will introduce a few controllers as benchmarks for comparison.

### A. Problem Formulation

Consider an MAS consisting of one leader and $N$ followers where the dynamics of agents are described as

$$\begin{cases} \dot{z}_0(t) = hz_0(t), \\ \dot{z}_i(t) = hz_i(t) + ku_i(t) + \Delta\rho_i(t), \ i = 1, 2, 3, ..., N. \end{cases} \tag{5}$$

Here, $z_0(t)$ is the state of the leader; $z_i(t)$ and $u_i(t)$ denote the state and the control input of agent $i$, respectively; $\Delta\rho_i(t)$ is the external noise; and $h \neq 0$ and $k \neq 0$ denote system parameters. The communication topology is denoted as $\hat{\mathcal{G}}$.

The assumptions provided below represent the standard conditions for MASs to achieve leader-follower consensus [33], [34].

*Assumption 1:* The pair $(h, k)$ is controllable.

*Assumption 2:* The communication topology graph $\hat{\mathcal{G}}$ of MAS (5) consists of a directed spanning tree that has the leader node as its root.

*Definition 1:* MAS (5) is said to achieve leader-follower consensus if the following conditions are met:

$$\lim_{t\to+\infty} \|z_i(t) - z_0(t)\| = 0, \quad i = 1, 2, ..., N, \quad \text{and}$$
$$\lim_{t\to+\infty} \|z_i(t) - z_j(t)\| = 0, \quad i, j = 1, 2, ..., N,$$

where $z_0(t)$ is the state of the leader, and $z_i(t)$ and $z_j(t)$ are the states of the followers in MAS (5).

According to *Definition 1*, to achieve the consensus, the state difference between each agent should gradually approach zero over time. In this case, the $i$th error function that measures the difference in states between the $i$th agent and other agents is defined as

$$e_i(t) = \sum_{j=1}^{N} \left(a_{ij}(z_i(t) - z_j(t)) + \hat{a}_i(z_i(t) - z_0(t))\right) \tag{6}$$

where $N$ is the number of followers in MAS (5), $a_{ij}$ denotes the $ij$-th element of $\mathcal{A}$, and $\hat{a}_i$ denotes the $ii$-th element of $\mathcal{A}'$.

Naturally, based on the communication topology $\hat{\mathcal{G}}$, the error function of the whole system is

$$\boldsymbol{e}(t) = (\mathcal{L} + \mathcal{A}')\boldsymbol{z}(t) - \mathcal{A}'(\mathbf{1}_N \otimes z_0(t)), \tag{7}$$

where $\boldsymbol{z}(t)$ denotes the state of the followers in MAS (5), $\mathbf{1}_N = [1; ...; 1] \in \mathbb{R}^N$, $N$ is the number of followers, and the symbol $\otimes$ represents the Kronecker product.

*Remark 2:* Under aforementioned assumptions, all the eigenvalues of the matrix $(\mathcal{L} + \mathcal{A}')$ have positive real parts [35].

### B. Design of NF-FNNC

In light of the neural network model in [18], a consensus state observer $\boldsymbol{\Theta}(t)$ with an integral unit is devised as

$$\boldsymbol{\Theta}(t) = \boldsymbol{e}(t) + \varsigma \int_0^t \Psi(\boldsymbol{e}(\iota))\mathrm{d}\iota, \tag{8}$$

where $\varsigma > 0$ denotes a fixed gain parameter, $\Psi(\cdot)$ is the proposed partition-sign-by-power activation function (PSBPAF), and the element of $\Psi(\cdot)$ is formed as

$$\psi(\tau) = \begin{cases} (\alpha_1|\tau|^{\kappa_1}\mathrm{sign}(\tau) + \alpha_2\tau)\exp\left(|\tau|^{\omega}\right) \\ \quad + \alpha_3\mathrm{sign}(\tau), & \text{if } |\tau| \leqslant 1, \\ (\alpha_1|\tau|^{\kappa_2}\mathrm{sign}(\tau) + \alpha_2\tau)\exp\left(|\tau|^{\omega}\right) \\ \quad + \alpha_3\mathrm{sign}(\tau), & \text{else,} \end{cases} \tag{9}$$

where $\alpha_1$, $\alpha_2$, and $\alpha_3$ are positive constants, $0 < \kappa_1 < 1$, $\kappa_2 > 1$, $0 < \omega < 1$, and $\mathrm{sign}(\cdot)$ is defined by

$$\mathrm{sign}(\tau) = \begin{cases} 1, \text{ if } \tau > 0, \\ 0, \text{ if } \tau = 0, \\ -1, \text{ if } \tau < 0. \end{cases} \tag{10}$$

Furthermore, the noise suppressor $\dot{\boldsymbol{\Theta}}(t)$ [36] which incorporates the fuzzy gain parameter generated by the TSFLS is formulated as

$$\dot{\boldsymbol{\Theta}}(t) = -\eta\Psi(\boldsymbol{\Theta}(t)) + \boldsymbol{\varrho}(t), \tag{11}$$

where

$$\eta = \frac{\sum_{i=1}^{n} w_i o_i}{\sum_{i=1}^{n} w_i}$$

is the fuzzy gain parameter as defined in (3), $\Psi(\cdot)$ is PSBPAF as in (9), and $\boldsymbol{\varrho}(t) = (\mathcal{L} + \mathcal{A}')\Delta\boldsymbol{\rho}(t)$ denotes the external noise.

*Remark 3:* The role of the noise suppressor is to gauge the fluctuating noise by leveraging dynamic information from the synchronization process. Essentially, the noise suppressor strives to ensure that $\eta\Psi(\boldsymbol{\Theta}(t))$ converges to $\boldsymbol{\varrho}(t)$.

Considering (5), (7), (8), and (11), the noise-tolerant fixed-time fuzzy neural network (NF-FNN) model is derived as

$$\begin{aligned} &(\mathcal{L} + \mathcal{A}')\left(h\boldsymbol{z}(t) + k\boldsymbol{u}(t) + \Delta\boldsymbol{\rho}(t)\right) - \mathcal{A}'(\mathbf{1}_N \otimes hz_0(t)) \\ &= -\varsigma\Psi(\boldsymbol{e}(t)) - \eta\Psi\left(\boldsymbol{e}(t) + \varsigma\int_0^t \Psi(\boldsymbol{e}(\iota))\mathrm{d}\iota\right) + \boldsymbol{\varrho}(t). \end{aligned} \tag{12}$$

Consequently, based on NF-FNN (12), the NF-FNNC for leader-follower consensus of MAS (5) is

$$\boldsymbol{u}(t) = \left(-h\boldsymbol{z}(t) + C\left(\boldsymbol{f}_1(t) + \boldsymbol{f}_2(t)\right)\right)/k, \tag{13}$$

where

$$\begin{aligned}
&C = (\mathcal{L} + \mathcal{A}')^{-1},\\
&\boldsymbol{f}_1(t) = -\varsigma\Psi(\boldsymbol{e}(t)) - \eta\Psi\left(\boldsymbol{e}(t) + \varsigma\int_0^t \Psi(\boldsymbol{e}(\iota))\mathrm{d}\iota\right),\\
&\boldsymbol{f}_2(t) = \mathcal{A}'(\mathbf{1}_N \otimes hz_0(t)).
\end{aligned}$$

### C. Controllers for Comparison

*1) Traditional controller (TraC) [8]:* The TraC of the $i$th agent for leader-follower consensus can be written as

$$\begin{aligned}
u_i(t) &= -\varsigma e_i(t)\\
&= -\varsigma\sum_{j=1}^{N}\left(a_{ij}(z_i(t) - z_j(t)) + \hat{a}_i(z_i(t) - z_0(t))\right),
\end{aligned} \tag{14}$$

where $\varsigma > 0$ denotes the fixed gain parameter. Hence, we obtain the following TraC:

$$\boldsymbol{u}(t) = -\varsigma\boldsymbol{e}(t). \tag{15}$$

*2) Exponential-bi-power distributed gradient neural network controller (EDGNNC) [10]:* The dynamics of the exponential-bi-power distributed gradient neural network (EDGNN) model [10] is

$$\dot{z}_i(t) = -\varsigma\exp(ce_i^r(t))e_i^p(t), \tag{16}$$

where $z_i(t)$ and $e_i(t)$ denote the state and the error function of the $i$th follower, respectively; $c > 0$, $r > 0$, and $0 < p < 1$ are constants. Based on (7) and (16), the EDGNN model for leader-follower consensus of MAS (5) is acquired as follows:

$$h\boldsymbol{z}(t) + k\boldsymbol{u}(t) + \varDelta\boldsymbol{\rho}(t) = -\varsigma\exp(c\boldsymbol{e}^r(t))\boldsymbol{e}^p(t). \tag{17}$$

Then, the EDGNNC based on the EDGNN model can be written as

$$\boldsymbol{u}(t) = \left(-h\boldsymbol{z}(t) - \varsigma\exp(c\boldsymbol{e}^r(t))\boldsymbol{e}^p(t)\right)/k. \tag{18}$$

*3) Novel ZNN controller (NZNNC) [18]:* Based on [18] and the modeling process of NF-FNN (12), the NZNN model for leader-follower consensus is

$$\begin{aligned}
&(\mathcal{L} + \mathcal{A}')\left(h\boldsymbol{z}(t) + k\boldsymbol{u}(t) + \varDelta\boldsymbol{\rho}(t)\right) - \mathcal{A}'(\mathbf{1}_N \otimes hz_0(t))\\
&\quad = -\varsigma\boldsymbol{e}(t) - \varsigma\left(\boldsymbol{e}(t) + \varsigma\int_0^t \boldsymbol{e}(\iota)\mathrm{d}\iota\right) + \boldsymbol{\varrho}(t).
\end{aligned} \tag{19}$$

Then, the NZNNC can be formulated as

$$\boldsymbol{u}(t) = \frac{\boldsymbol{z}(t) + C(\boldsymbol{f}_{1n}(t) + \boldsymbol{f}_{2n}(t))}{k}, \tag{20}$$

where

$$\begin{aligned}
&C = (\mathcal{L} + \mathcal{A}')^{-1},\\
&\boldsymbol{f}_{1n}(t) = -\varsigma\boldsymbol{e}(t) - \varsigma\left(\boldsymbol{e}(t) + \varsigma\int_0^t \boldsymbol{e}(\iota)\mathrm{d}\iota\right),\\
&\boldsymbol{f}_{2n}(t) = \mathcal{A}'(\mathbf{1}_N \otimes hz_0(t)).
\end{aligned}$$

*4) Novel Fuzzy-Neural-Network controller (NFNNC):* Analogously, introducing a fuzzy gain parameter to NZNN model (19), the novel fuzzy neural network (NFNN) model for leader-follower consensus can be expressed as

$$\begin{aligned}
&(\mathcal{L} + \mathcal{A}')\left(h\boldsymbol{z}(t) + k\boldsymbol{u}(t) + \varDelta\boldsymbol{\rho}(t)\right) - \mathcal{A}'({}_N \otimes hz_0(t))\\
&\quad = -\varsigma\boldsymbol{e}(t) - \eta\left(\boldsymbol{e}(t) + \varsigma\int_0^t \boldsymbol{e}(\iota)\mathrm{d}\iota\right) + \boldsymbol{\varrho}(t),
\end{aligned} \tag{21}$$

where

$$\eta = \frac{\sum_{i=1}^{n} w_i o_i)}{\sum_{i=1}^{n} w_i}$$

denotes the fuzzy gain parameter as defined in (3). Then, the NFNNC obtained by the NFNN model can be represented as

$$\boldsymbol{u}(t) = \frac{-h\boldsymbol{z}(t) + C\left(\boldsymbol{f}_{1f}(t) + \boldsymbol{f}_{2f}(t)\right)}{k} \tag{22}$$

where

$$\begin{aligned}
&C = (\mathcal{L} + \mathcal{A}')^{-1},\\
&\boldsymbol{f}_{1f}(t) = -\varsigma\boldsymbol{e}(t) - \eta\left(\boldsymbol{e}(t) + \varsigma\int_0^t \boldsymbol{e}(\iota)\mathrm{d}\iota\right),\\
&\boldsymbol{f}_{2f}(t) = \mathcal{A}'(\mathbf{1}_N \otimes hz_0(t)).
\end{aligned}$$

## IV. Theoretical Analysis

In this section, we present two theorems about the NF-FNNC. Through rigorous mathematical analysis, these theorems highlight the fixed-time stability and enhanced noise-tolerance of the designed NF-FNNC.

*Theorem 1:* Under noise-free conditions, NF-FNNC (13) can make MAS (5) achieve leader-follower consensus in fixed time $\hat{T}$ whose upper bound satisfies

$$\hat{T} \leqslant \frac{\eta + \varsigma}{\eta\varsigma}\left(\frac{\ln\left(1 + \frac{\alpha_2}{\alpha_1}\right)}{\alpha_2(1 - \kappa_1)} + \frac{\ln\left(1 + \frac{\alpha_2}{\alpha_1}\right)}{\alpha_2\exp(1)(\kappa_2 - 1)}\right), \tag{23}$$

where $\eta$, $\varsigma$, $\alpha_1$, $\alpha_2$, $\kappa_1$, and $\kappa_2$ are defined previously.

*Proof:* Clearly, the MAS achieves leader-follower consensus when NF-FNN model (12) is stable. First, the NF-FNN model can be written as

$$\dot{\boldsymbol{e}}(t) = \dot{\boldsymbol{\Theta}}(t) - \varsigma\Psi(\boldsymbol{e}(t)) \tag{24}$$

where $\dot{\boldsymbol{\Theta}}(t)$ is the noise suppressor satisfying (11). Evidently, it is challenging to analyze the stabilization time of system (24) directly. In this case, it makes sense to consider the stabilization time for $\dot{\boldsymbol{\Theta}}(t)$ to reach 0.

We start by dealing with the noise-free case and the noise suppressor $\dot{\boldsymbol{\Theta}}(t) = -\eta\Psi(\boldsymbol{\Theta}(t)) + \boldsymbol{\varrho}(t)$ in element wise is characterized as follows:

$$\dot{\theta}_i(t) = -\eta\psi(\theta_i(t)) \tag{25}$$

where $\dot{\theta}_i(t)$ and $\theta_i(t)$ represent the $i$th element of $\dot{\boldsymbol{\Theta}}(t)$ and $\boldsymbol{\Theta}(t)$, respectively.

Next, define a Lyapunov function candidate:

$$\ell_i(t) = |\theta_i(t)|. \tag{26}$$

Taking the time derivative of $\ell_i(t)$, we obtain

$$\begin{aligned}\dot{\ell}_i(t) &= \operatorname{sign}(\theta_i(t))\dot{\theta}_i(t)\\ &= \operatorname{sign}(\theta_i(t))\left(-\eta\psi(\theta_i(t))\right).\end{aligned} \tag{27}$$

According to the segmented nature of PSBPAF (9), it is necessary to divide the subsequent proof into two cases according to the abstract value of $\theta_i(0)$: one is the case when $|\theta_i(0)| > 1$; and the other is the case when $|\theta_i(0)| \leq 1$.

*Case 1*: $|\theta_i(0)| > 1$. In this case, the stabilization time consists of two parts: one is the time that $|\theta_i(t)|$ takes to drop from $|\theta_i(0)|$ to 1; and the other is the time that it takes from 1 to 0. Denote these two parts by $t_1$ and $t_2$, respectively.

1) Let us calculate $t_1$ firstly. Considering PSBPAF (9), (27) can be reformulated as

$$\begin{aligned}\dot{\ell}_i(t) = {} & \operatorname{sign}(\theta_i(t))\big(-\eta\alpha_3\operatorname{sign}(\theta_i(t))\\ & -\eta\big(\alpha_1|\theta_i(t)|^{\kappa_2}\operatorname{sign}(\theta_i(t)) + \alpha_2\theta_i(t)\big)\exp\left(|\theta_i(t)|^{\omega}\right)\big)\\ = {} & -\eta\big(\alpha_3 + \big(\alpha_1|\theta_i(t)|^{\kappa_2} + \alpha_2|\theta_i(t)|\big)\exp\left(|\theta_i(t)|^{\omega}\right)\big)\\ < {} & -\eta\exp\left(|\theta_i(t)|^{\omega}\right)\big(\alpha_1|\theta_i(t)|^{\kappa_2} + \alpha_2|\theta_i(t)|\big)\\ \leqslant {} & -\eta\alpha_1\ell_i^{\kappa_2}(t)\exp(1) - \eta\alpha_2\ell_i(t)\exp(1).\end{aligned} \tag{28}$$

Consequently, we have $\ell_i(t) \geqslant 0$ and $\dot{\ell}_i(t) < 0$, leading to the conclusion that (25) is Lyapunov stable. Furthermore, the maximum stabilization time $t_1$ can be calculated as follows by utilizing *Lemma 1*:

$$\begin{aligned}t_1 &\leqslant \frac{\ln\left(1 + \frac{\eta\alpha_2\exp(1)\left(1-\ell_i^{1-\kappa_2}(0)\right)}{\eta\alpha_2\exp(1)\ell_i^{1-\kappa_2}(0)+\eta\alpha_1\exp(1)}\right)}{\eta\alpha_2\exp(1)(\kappa_2-1)}\\ &= \frac{\ln\left(1 + \frac{\alpha_2\left(1-\ell_i^{1-\kappa_2}(0)\right)}{\alpha_2\ell_i^{1-\kappa_2}(0)+\alpha_1}\right)}{\eta\alpha_2\exp(1)(\kappa_2-1)}\\ &< \frac{\ln\left(1+\frac{\alpha_2}{\alpha_1}\right)}{\eta\alpha_2\exp(1)(\kappa_2-1)}.\end{aligned} \tag{29}$$

2) Next, we calculate the stabilization time $t_2$. Based on PSBPAF (9), (27) can be represented as

$$\begin{aligned}\dot{\ell}_i(t) = {} & \operatorname{sign}(\theta_i(t))\left(-\eta\alpha_3\operatorname{sign}(\theta_i(t))\right.\\ & \left.-\eta\left(\alpha_1|\theta_i(t)|^{\kappa_1}\operatorname{sign}(\theta_i(t)) + \alpha_2\theta_i(t)\right)\exp\left(|\theta_i(t)|^{\omega}\right)\right)\\ = {} & -\eta\left(\alpha_3 + \left(\alpha_1|\theta_i(t)|^{\kappa_1} + \alpha_2|\theta_i(t)|\right)\exp\left(|\theta_i(t)|^{\omega}\right)\right)\\ < {} & -\eta\alpha_1\ell_i^{\kappa_1}(t) - \eta\alpha_2\ell_i(t).\end{aligned} \tag{30}$$

Similarly, the Lyapunov stability can also be deduced in this case according to the facts of $\ell_i(t) \geqslant 0$ in (26) and $\dot{\ell}_i(t) < 0$ in (30). Furthermore, an upper bound for stabilization time $t_2$ can be calculated as follows based on *Lemma 2*:

$$t_2 \leqslant \frac{\ln\left(1 + \frac{\eta\alpha_2}{\eta\alpha_1}\ell_i^{1-\kappa_1}(0)\right)}{\eta\alpha_2(1-\kappa_1)} \leqslant \frac{\ln\left(1+\frac{\alpha_2}{\alpha_1}\right)}{\eta\alpha_2(1-\kappa_1)}. \tag{31}$$

Concluding the above discussion, when $|\theta_i(0)| > 1$, the stabilization time satisfies

$$\begin{aligned}T_{1i} &= t_1 + t_2\\ &< \frac{\ln\left(1+\frac{\alpha_2}{\alpha_2+\alpha_1}\right)}{\eta\alpha_2\exp(1)(\kappa_2-1)} + \frac{\ln\left(1+\frac{\alpha_2}{\alpha_1}\right)}{\eta\alpha_2(1-\kappa_1)}.\end{aligned} \tag{32}$$

*Case 2*: $|\theta_i(0)| \leqslant 1$. In this case, the stabilization time is certainly equal to or less than $t_2$, and the stabilization time of $\theta_i(t)$ converges from 1 to 0, which still adheres to the stabilization time upper bound $T_{1i}$.

From the aforementioned discussion, we know that $\theta_i(t) = 0$ when $t \geqslant T_{1i}$. Thus, (24) can be reformulated as

$$\dot{e}_i(t) = -\varsigma\psi(e_i(t)) \tag{33}$$

where $t \geqslant T_{1i}$.

The expressions of $\dot{e}_i(t)$ in (33) and $\dot{\theta}_i(t)$ in (25) only differ in the gain parameters, and (8) indicates that $e_i(0) = \theta_i(0)$. Consequently, the stabilization time $T_{2i}$ of (33) can be calculated by a similar method as in *Case 1*, which gives

$$T_{2i} < \frac{\ln\left(1+\frac{\alpha_2}{\alpha_1}\right)}{\varsigma\alpha_2(1-\kappa_1)} + \frac{\ln\left(1+\frac{\alpha_2}{\alpha_1}\right)}{\varsigma\alpha_2\exp(1)(\kappa_2-1)}. \tag{34}$$

Summarizing the analysis conducted so far, we obtain the stabilization time $T_i$ of $i$th subsystem as

$$T_i = T_{1i} + T_{2i} \tag{35}$$

which confirms that the NF-FNNC achieves the leader-follower consensus for the MAS (5) within a fixed time of $\hat{T}$ calculated by:

$$\begin{aligned}\hat{T} &= \max\{T_i\}\\ &< \frac{\eta+\varsigma}{\eta\varsigma}\left(\frac{\ln\left(1+\frac{\alpha_2}{\alpha_1}\right)}{\alpha_2(1-\kappa_1)} + \frac{\ln\left(1+\frac{\alpha_2}{\alpha_1}\right)}{\alpha_2\exp(1)(\kappa_2-1)}\right).\end{aligned} \tag{36}$$

Note that the upper bound of stabilization time $\hat{T}$ is not influenced by the initial state of MAS (5) but, instead, is dependent solely on the parameters of the NF-FNNC. The proof is now complete. ■

*Theorem 2:* Consider the external noise $\boldsymbol{\varrho}(t)$ satisfying $|\varrho_i(t)| < \eta\alpha_3$. Then, under NF-FNNC (13), MAS (5) achieves the leader-follower consensus in a fixed time of $\hat{T}$ whose upper bound satisfies

$$\hat{T} \leqslant \frac{\eta+\varsigma}{\eta\varsigma}\left(\frac{\ln\left(1+\frac{\alpha_2}{\alpha_1}\right)}{\alpha_2(1-\kappa_1)} + \frac{\ln\left(1+\frac{\alpha_2}{\alpha_1}\right)}{\alpha_2\exp(1)(\kappa_2-1)}\right). \tag{37}$$

*Proof:* Similar to *Theorem 1*, we can calculate the stabilization time for $\boldsymbol{\Theta}(t)$ to approach 0 by considering (24) firstly. In this case, the $i$th subsystem corresponding to (11) is

$$\dot{\theta}_i(t) = -\eta\psi(\theta_i(t)) + \varrho_i(t) \tag{38}$$

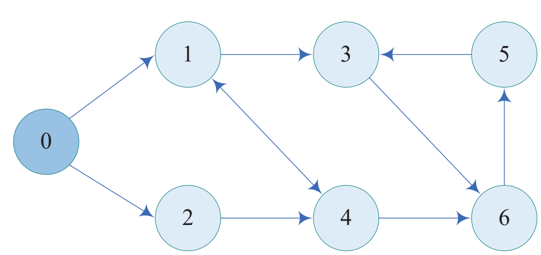


Fig. 3. Communication topology of MAS (5).

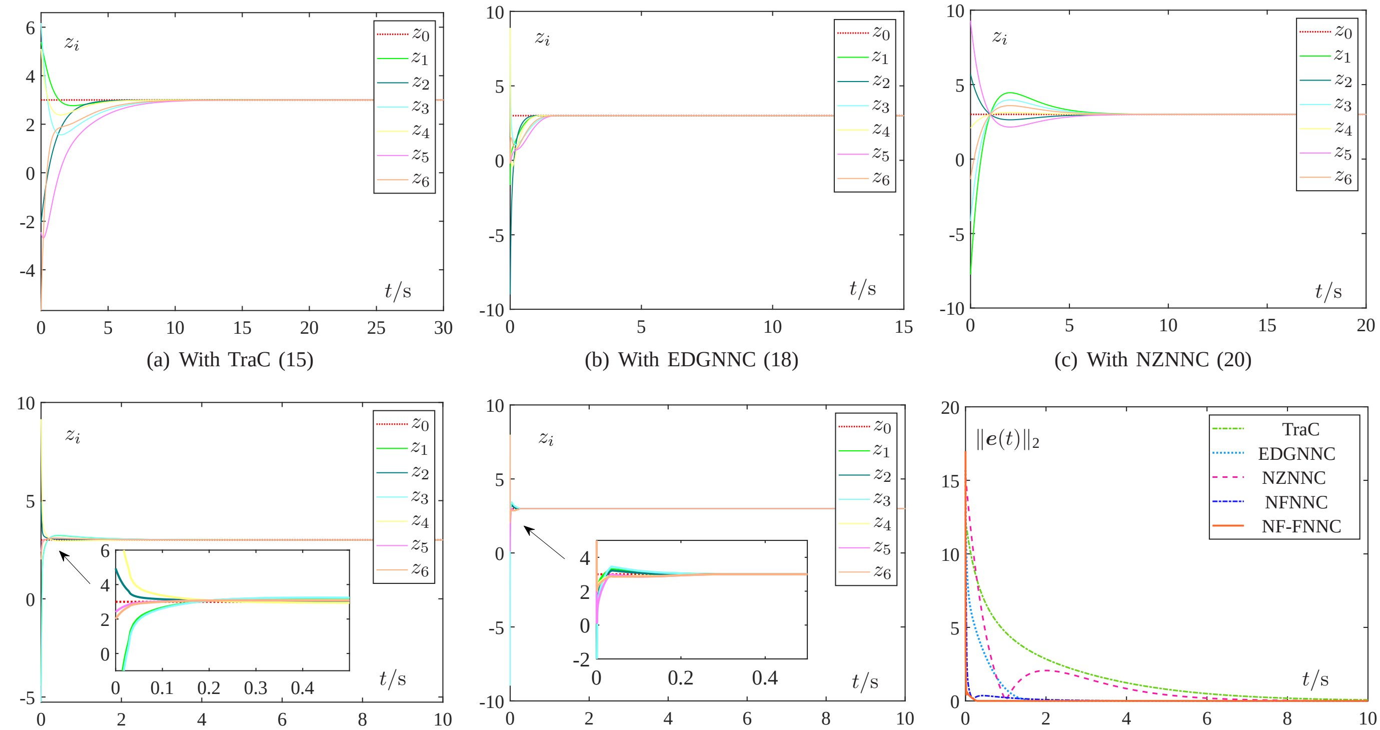


(a) With TraC (15)
(b) With EDGNNC (18)
(c) With NZNNC (20)
(d) With NFNNC (22)
(e) With NF-FNNC (13)
(f) Errors in the MAS

Fig. 4. States and errors of the MAS defined in *Example 1* with different control methods when $z_0(t) = 3$.

where $\varrho_i(t)$ represents the external noise. Then, define a Lyapunov function for System (38) as

$$\ell_i(t) = |\theta_i(t)|^2. \tag{39}$$

Combining with (38), the time derivative of (39) is computed as follows:

$$\begin{aligned}\dot{\ell}_i(t) &= 2\theta_i(t)\dot{\theta}_i(t)\\ &= 2\theta_i(t)\left(-\eta\psi(\theta_i(t)) + \varrho_i(t)\right).\end{aligned} \tag{40}$$

Similar to the proof of *Theorem 1*, we consider two cases for (40) because of the segmented nature of PSBPAF (9).

We first discuss the case $|\theta_i(0)| > 1$, in which the stabilization time consists of two parts: one is the time that $|\theta_i(0)|$ takes to drop from $|\theta_i(0)|$ to 1, denoted by $t_1$; and the other is the time that $|\theta_i(0)|$ needs to drop from 1 to 0, denoted by $t_2$.

1) We calculate $t_1$ first. Taking PSBPAF (9) into consideration, (40) can be expressed as

$$\begin{aligned}\dot{\ell}_i(t) =\ & 2\theta_i(t)\Big(\varrho_i(t) - \eta\big(\alpha_3\mathrm{sign}(\theta_i(t))\\ &+ \left(\alpha_1|\theta_i(t)|^{\kappa_2}\mathrm{sign}(\theta_i(t)) + \alpha_2\theta_i(t)\right)\exp\left(|\theta_i(t)|^{\omega}\right)\big)\Big)\\ =\ & 2\theta_i(t)\varrho_i(t) - 2\eta\alpha_1|\theta_i(t)|^{1+\kappa_2}\exp\left(|\theta_i(t)|^{\omega}\right)\\ &- 2\eta\alpha_2|\theta_i(t)|^2\exp\left(|\theta_i(t)|^{\omega}\right) - 2\eta\alpha_3|\theta_i(t)|\\ \leqslant\ & 2\left(|\theta_i(t)||\varrho_i(t)| - \eta\alpha_3|\theta_i(t)|\right)\\ &- 2\eta\exp\left(|\theta_i(t)|^{\omega}\right)\left(\alpha_1|\theta_i(t)|^{1+\kappa_2} + \alpha_2|\theta_i(t)|^2\right).\end{aligned} \tag{41}$$

Additionally, under the condition $|\varrho_i(t)| \leqslant \eta\alpha_3$, (41) can be expressed more explicitly as

$$\begin{aligned}\dot{\ell}(t) &\leqslant 2\eta\exp\left(|\theta_i(t)|^{\frac{\omega}{2}}\right)\left(\alpha_1\ell_i^{\frac{1+\kappa_2}{2}}(t) + \alpha_2\ell_i(t)\right)\\ &< -2\eta\alpha_1\exp(1)\ell_i^{\frac{1+\kappa_2}{2}}(t) - 2\eta\alpha_2\exp(1)\ell_i(t).\end{aligned} \tag{42}$$

Consequently, according to *Lemma 1*, the upper bound of time for $|\theta_i(t)|$ converging to 1 is

$$\begin{aligned}t_1 &\leqslant \frac{\ln\left(1 + \frac{\eta\alpha_2\exp(1)\left(1-\ell_i^{1-\kappa_2}(0)\right)}{\eta\alpha_2\exp(1)\ell_i^{1-\kappa_2}(0)+\eta\alpha_1\exp(1)}\right)}{\eta\alpha_2\exp(1)(\kappa_2-1)}\\ &= \frac{\ln\left(1 + \frac{\alpha_2\left(1-\ell_i^{1-\kappa_2}(0)\right)}{\alpha_2\ell_i^{1-\kappa_2}(0)+\alpha_1}\right)}{\eta\alpha_2\exp(1)(\kappa_2-1)}\\ &< \frac{\ln\left(1+\frac{\alpha_2}{\alpha_1}\right)}{\eta\alpha_2\exp(1)(\kappa_2-1)}.\end{aligned} \tag{43}$$

2) Next, we calculate $t_2$. In this case, (40) can be reformulated as

$$\begin{aligned}\dot{\ell}(t) &< 2\eta\exp\left(|\theta_i(t)|^{\frac{\omega}{2}}\right)\left(\alpha_1\ell_i^{\frac{1+\kappa_1}{2}}(t) + \alpha_2\ell_i(t)\right)\\ &< -2\eta\alpha_1\ell_i^{\frac{1+\kappa_1}{2}}(t) - 2\eta\alpha_2\ell_i(t).\end{aligned} \tag{44}$$

Analogously, the upper bound of $t_2$ for $|\theta_i(t)|$ to drop from 1 to 0 can be calculated as follows on the basis of *Lemma 2*:

$$t_2 < \frac{\ln\left(1+\frac{\eta\alpha_2}{\eta\alpha_1}\ell_i^{1-\kappa_1}(0)\right)}{\eta\alpha_2(1-\kappa_1)} < \frac{\ln\left(1+\frac{\alpha_2}{\alpha_1}\right)}{\eta\alpha_2(1-\kappa_1)}. \tag{45}$$

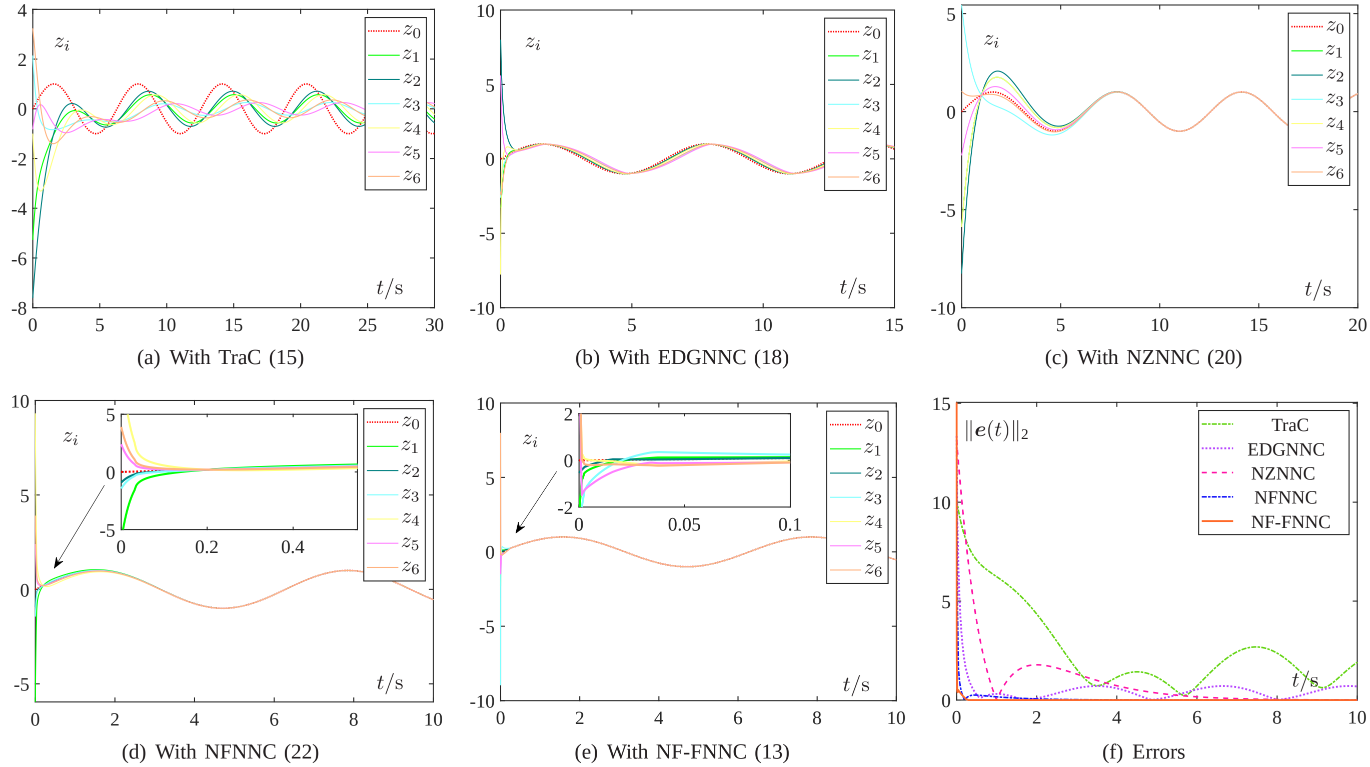


(a) With TraC (15)
(b) With EDGNNC (18)
(c) With NZNNC (20)
(d) With NFNNC (22)
(e) With NF-FNNC (13)
(f) Errors

Fig. 5. States and errors of the MAS defined in *Example 1* with different control methods when $z_0(t) = \sin(t)$.

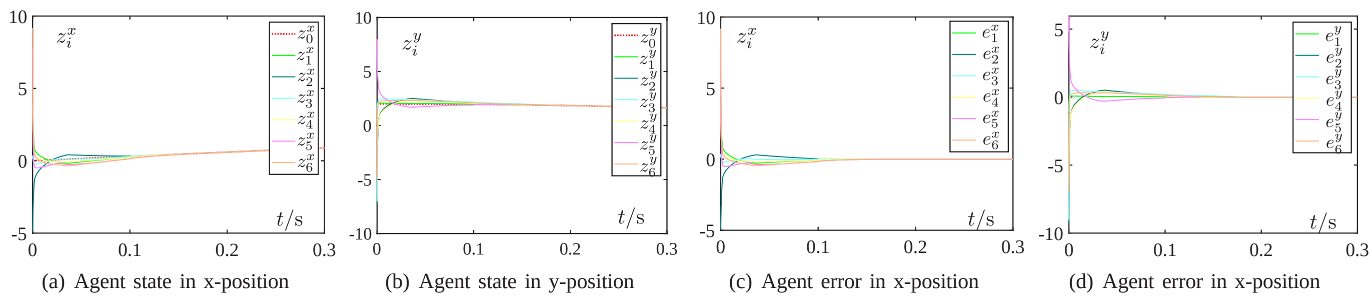


(a) Agent state in x-position
(b) Agent state in y-position
(c) Agent error in x-position
(d) Agent error in x-position

Fig. 6. States and errors of the MAS defined in *Example 2* with NF-FNNC (13) when $z_0(t) = (3\sin(t), 2\cos(2t))$.

Therefore, when $\theta_i(0) > 1$, the stabilization time $T_{1i}$ is

$$\begin{aligned} T_{1i} &= t_1 + t_2 \\ &< \frac{\ln\left(1 + \frac{\alpha_2}{\alpha_1}\right)}{\eta\alpha_2 \exp(1)(\kappa_2 - 1)} + \frac{\ln\left(1 + \frac{\alpha_2}{\alpha_1}\right)}{\eta\alpha_2(1 - \kappa_1)}. \end{aligned} \tag{46}$$

Now, we are in a position to discuss the case of $|\theta_i(0)| \leqslant 1$. In this case, the stabilization time is certainly less than or equal to $t_2$, which is the stabilization time of $\theta_i(t)$ (converging from 1 to 0) having an upper bound of $T_{1i}$. Based on the previous analysis, we know that $\theta_i(t) = 0$ is stable when $t \geqslant T_{1i}$. In addition, we can deduce from (24) that, when $t \geqslant T_{1i}$, system $\dot{e}_i(t) = -\varsigma\psi(e_i(t))$ is stable if and only if MAS (5) reaches leader-follower consensus. Accordingly, the stabilization time of $\dot{e}_i(t) = -\varsigma\psi(e_i(t))$ can be calculated along a similar line to the proof of *Theorem 1*, and is thus omitted here. In particular, $T_{2i}$ satisfies

$$T_{2i} < \frac{\ln\left(1 + \frac{\alpha_2}{\alpha_1}\right)}{\varsigma\alpha_2(1 - \kappa_1)} + \frac{\ln\left(1 + \frac{\alpha_2}{\alpha_1}\right)}{\varsigma\alpha_2 \exp(1)(\kappa_2 - 1)}. \tag{47}$$

To this end, we conclude that the $i$th subsystem is stable within the time period $T_i$ with $T_i = T_{1i} + T_{2i}$. Overall, MAS (5) can reach the leader-follower consensus under the control of NF-FNNC in the presence of the external noise within a fixed time of $\hat{T}$: $\hat{T} = \max\{T_i\} = \max\{T_{1i} + T_{2i}\}$

$$= \frac{\eta + \varsigma}{\eta\varsigma}\left(\frac{\ln\left(1 + \frac{\alpha_2}{\alpha_1}\right)}{\alpha_2(1 - \kappa_1)} + \frac{\ln\left(1 + \frac{\alpha_2}{\alpha_1}\right)}{\alpha_2 \exp(1)(\kappa_2 - 1)}\right),$$

and this ends the proof. ■

*Remark 4:* In Theorems 1 and 2, we have delved into an NF-FNNC enhanced with the TSFLS to tackle the leader-follower consensus problem in MASs. The integration of an error integral term during the NF-FNNC's formulation boosts

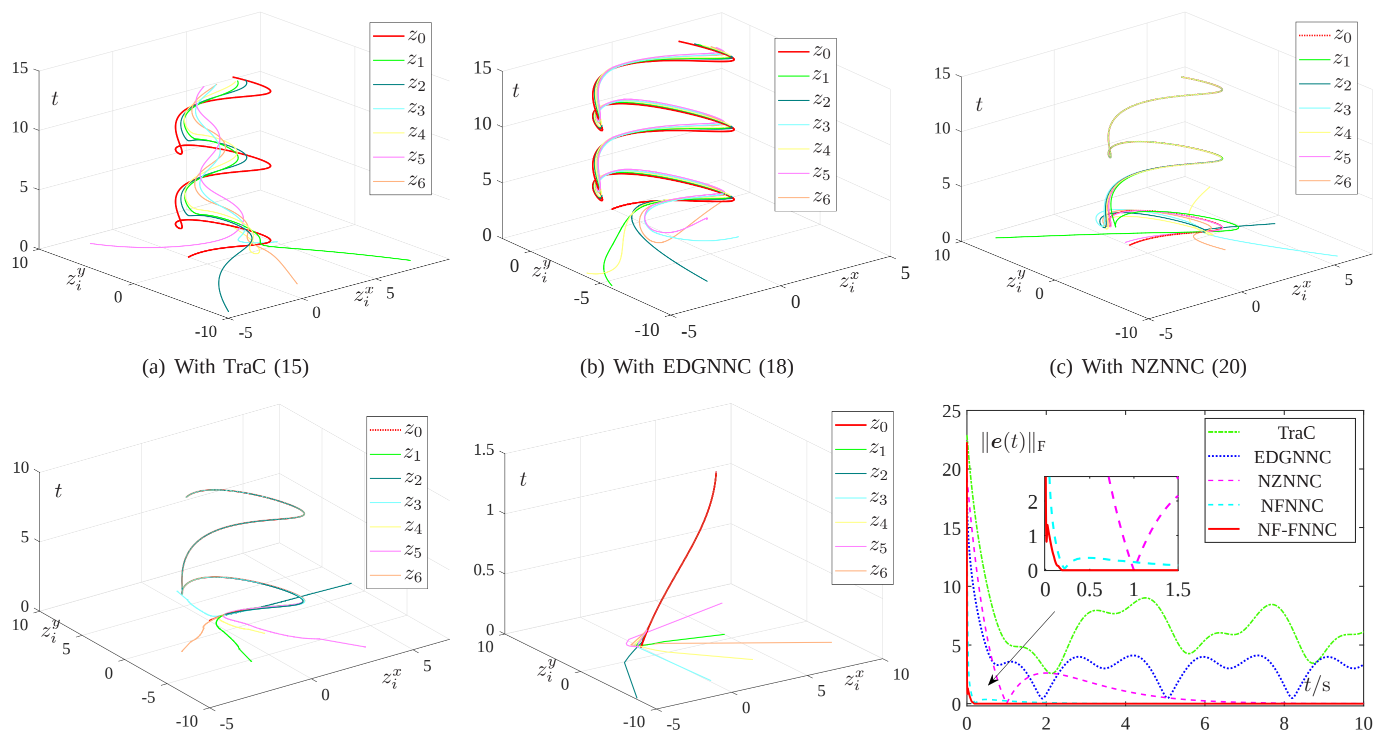


(a) With TraC (15) (b) With EDGNNC (18) (c) With NZNNC (20)

(d) With NFNNC (22) (e) With NF-FNNC (13) (f) Errors

Fig. 7. States and errors of the MAS defined in *Example 2* with different control methods when $z_0(t) = (3\sin(t), 2\cos(2t))$.

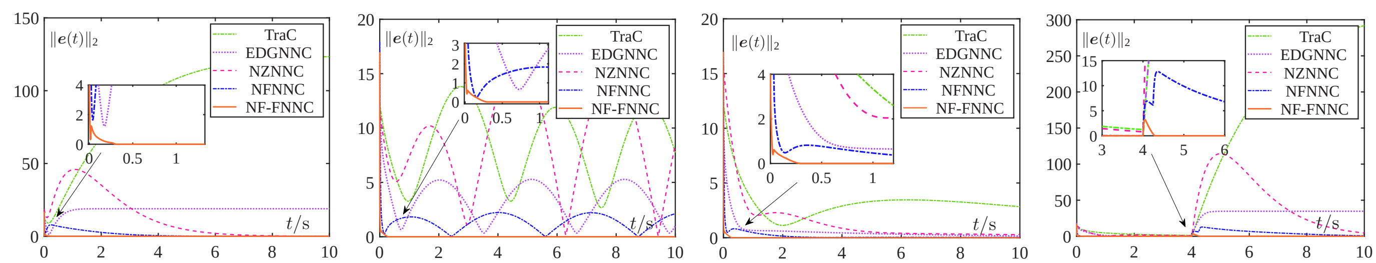


(a) With noise $\varrho_i(t) = 20$ (b) With noise $\varrho_i(t) = 5\sin(t)$ (c) With noise $\varrho_i(t) = \exp(-0.1t)$ (d) With $\varrho_i(t) = 50$ after 4 seconds

Fig. 8. Comparison of errors in the MAS defined in *Example 3* with different external noises when $z_0(t) = 3$.

its resistance to noise. Concurrently, the application of a fuzzy gain parameter, derived from the TSFLS, equips the NF-FNNC with adaptive control capabilities. We have also incorporated a newly devised PSBPAF in the NF-FNNC, ensuring that the MAS reaches consensus within a set time span with its upper bound calculated in Theorems 1 and 2. Theoretical evaluations have highlighted the time-bound stability and robustness of the NF-FNNC, offering a more relaxed upper limit for its stabilization duration. In next section, we will use comprehensive numerical tests to further amplify the advantages of the NF-FNNC, particularly its swift convergence and notable noise resilience, outperforming alternative control strategies.

*Remark 5:* The leader-follower consensus control problem for MASs has recently drawn a great deal of research attention with a rich body literature available. In comparison to the existing results, the consensus algorithm proposed in this paper exhibits the following distinct novelties: 1) the NF-FNNCA is specifically designed to accommodate the requirements of noise-tolerance within a fixed time, and this represents the first time the ZNN method has been applied to address leader-follower consensus challenges; 2) by the proposed PSBPAF, quicker stabilization within a fixed-time frame is achieved by the NF-FNNC compared to other methods; 3) the gain parameter of the NF-FNNC is dynamically adjusted using the TSFLS, resulting in enhanced adaptive robustness; and 4) the fixed-time stability and noise resilience of systems using the proposed NF-FNNC are confirmed through comprehensive theoretical analysis, and the superior efficacy of the method in managing the leader-follower consensus within MASs is validated by numerical simulations.

## V. Numerical Simulation

In this section, we present a series of numerical simulations to validate the effectiveness, rapid fixed-time stability, and robustness of the proposed NF-FNNC. Additionally, the performance of the NF-FNNC is compared with several controllers mentioned in Section III. In this part, $\alpha_1 = 1$, $\alpha_2 = 1$, $\alpha_3 = 1$, $\kappa_1 = 0.2$, $\kappa_2 = 2$, and $\omega = 0.5$ in PSBPAF (9). The fixed gain parameter is set as $\varsigma = 1$, and the fuzzy gain parameter is set as $\eta \in [10, 80]$. Additionally, $c = 2$, $r = 0.5$, and $p = 0.5$ in EDGNNC (18). The considered MAS has one leader and $6$ followers, of which the communication structure $\hat{\mathcal{G}}$ is exhibited in Fig. 3.

### A. Example 1

Consider two situations: 1) the leader has a fixed state of $z_0(t) = 3$; and 2) the leader has a time-varying state of $z_0(t) = \sin(t)$. As for followers in the MAS, the initial states $z_i(0), i \in \{1, 2, \cdots, 6\}$ are randomly generated in $[-10, 10]$.

States and system errors of the MAS controlled by the aforementioned controllers are illustrated in Figs. 4 and 5. Thereinto, the results depicted in Fig. 4 display that with the NF-FNNC, the MAS can reach leader-follower consensus in the shortest time, while with other controllers, it takes a relatively long time for the MAS to reach consensus. In Fig. 5, the NF-FNNC still makes the MAS with a dynamic leader achieve consensus fastest, while TraC (15) and EDGNNC (18) cannot make the MAS reach a consensus in this case. In conclusion, the superior control performance to other controllers of NF-FNNC with a fuzzy gain parameter and the state-of-the-art PSBPAF is demonstrated.

### B. Example 2

In this example, a more complex consensus problem of the MAS on a plane is considered. Consequently, states $z_i^x(t)$ and $z_i^y(t)$ are employed to describe the position information of the $i$th agent in x-direction and y-direction. The state of the leader is $z_0(t) = (z_0^x(t), z_0^x(t)) = (3\sin(t), 2\cos(2t))$, and the initial position states $z_i(0)$ of the followers are randomly generated in $[-10, 10]$.

Figure 6 reveals that under the control of NF-FNNC, the position of followers in the MAS can be synchronized to the position of the leader in a short time, that is, the MAS quickly reaches a consensus state. From Figs. 7(a)-7(e), trajectories of each agent in the MAS under different control methods can be observed, wherein the NF-FNNC can make each agent achieve a consensus with the leader in the fastest time. In contrast, other control methods fail to achieve leader-follower consensus of the MAS or require a significant amount of time to reach consensus. Furthermore, Fig. 7(f) exhibits the error variation of each controller. As shown, the error of NF-FNNC converges to zero fastest, which reflects the superior performance of NF-FNNC in this case.

### C. Example 3

The attainment of consensus for MAS can be easily disrupted by external noises. Hence, noise resilience is of paramount importance for a consensus protocol. Significantly, the NF-FNNC introduced in this study boasts potent noise resistance, enabling the MAS to achieve leader-follower consensus swiftly, even in the face of substantial external noise. Subsequent numerical simulations will attest to the noise tolerance capabilities of the NF-FNNC. In these simulations, the leader retains a constant state, while the initial states $z_i(0)$ of the $6$ followers are randomly generated in $[-10, 10]$.

As shown in Fig. 8, variation of system error with different controllers is displayed under four kinds of external noises: $\varrho_i(t) = 20$; $\varrho_i(t) = 5\sin(t)$; $\varrho_i(t) = \exp(-0.1t)$; and $\varrho_i(t) = 50$ that only appears when $t \geqslant 4$. Notably, results in Fig. 8 evidence that only NF-FNNC (13) can make the MAS achieve consensus ideally, which demonstrates the superior noise-tolerance of NF-FNNC. In contrast, other controllers for comparison cannot make the system reach stable effectively, and it is evident that they do not have a satisfactory ability to suppress noises.

## VI. Conclusion

In this paper, a noise-tolerant fixed-time fuzzy-neural-network controller has been proposed for the leader-follower consensus of a class of MASs, which incorporates the advantages of the zeroing neural network method in real-time control problems and the adaptive control performance of Takagi-Sugeno fuzzy logic systems. Several theorems have validated the fixed-time stability and excellent noise tolerance of the NF-FNNC. In particular, simulations have demonstrated that the proposed NF-FNNC has a shorter stabilization time and spectacular noise tolerance performance than other consensus controllers. Moreover, the NF-FNNC has consistently outperformed other methods under various external noise disturbances. In conclusion, the NF-FNNC is novel and effective, which provides a new method for the leader-follower consensus control of the MAS.

## References

[1] F. Yao, Y. Ding, S. Hong, and S.-H. Yang, "A survey on evolved LoRa-Based communication technologies for emerging internet of things applications," *Int. J. Netw. Dyn. Intell.*, pp. 4–19, 12 2022.

[2] H. Wang, Y. Tian, and H. Xu, "Neural adaptive command filtered control for cooperative path following of multiple underactuated autonomous underwater vehicles along one path," *IEEE Trans. Syst., Man, Cybern., Syst.*, vol. 52, no. 5, pp. 2966–2978, 2022.

[3] Y. Su, H. Cai, and J. Huang, "The cooperative output regulation by the distributed observer approach," *Int. J. Netw. Dyn. Intell.*, pp. 20–35, 2022.

[4] M. Lu and L. Liu, "Leader-following consensus of multiple uncertain Euler–Lagrange systems with unknown dynamic leader," *IEEE Trans. Autom. Control*, vol. 64, no. 10, pp. 4167–4173, 2019.

[5] C. Song and Y. Fan, "Coverage control for mobile sensor networks with limited communication ranges on a circle," *Automatica*, vol. 92, pp. 155–161, 2019.

[6] X. Dong, B. Yu, Z. Shi, and Y. Zhong, "Time-varying formation control for unmanned aerial vehicles: Theories and applications," *IEEE Trans. Control Syst. Technol.*, vol. 23, no. 1, pp. 340–348, 2015.

[7] H. J. Savino, C. R. dos Santos, F. O. Souza, L. C. Pimenta, M. De Oliveira, and R. M. Palhares, "Conditions for consensus of multi-agent systems with time-delays and uncertain switching topology," *IEEE Trans. Ind. Electron.*, vol. 63, no. 2, pp. 1258–1267, 2016.

[8] W. He, B. Xu, Q. L. Han, and F. Qian, "Adaptive consensus control of linear multiagent systems with dynamic event-triggered strategies," *IEEE Trans. Cybern.*, vol. 50, no. 7, pp. 2996–3008, 2020.

[9] Y. H. Choi and S. J. Yoo, "Neural-network-based distributed asynchronous event-triggered consensus tracking of a class of uncertain nonlinear multi-agent systems," *IEEE Trans. Neural Netw. Learn. Syst.*, vol. 33, no. 7, pp. 2965–2979, 2022.

[10] L. Xiao, L. Jia, J. Dai, Y. Cao, Y. Li, Q. Zhu, J. Li, and M. Liu, "Design and analysis of a novel distributed gradient neural network for solving consensus problems in a predefined time," *IEEE Trans. Neural Netw. Learn. Syst.*, 2022, in press with doi: 10.1109/TNNLS.2022.3193429.

[11] J. P. Mishra, C. Li, M. Jalili, and X. Yu, "Robust second-order consensus using a fixed-time convergent sliding surface in multiagent systems," *IEEE Trans. Cybern.*, vol. 50, no. 2, pp. 846–855, 2020.

[12] G. Wang, Z. Hao, B. Zhang, and L. Jin, "Convergence and robustness of bounded recurrent neural networks for solving dynamic Lyapunov equations," *Inf. Sci.*, vol. 588, pp. 106–123, 2022.

[13] J. Yan, L. Jin, X. Luo, and S. Li, "Modified RNN for solving comprehensive Sylvester equation with TDOA application," *IEEE Trans. Neural Netw. Learn. Syst.*, 2023, in press with doi: 10.1109/TNNLS.2023.3263565.

[14] Y. Zhang and S. S. Ge, "Design and analysis of a general recurrent neural network model for time-varying matrix inversion," *IEEE Trans. Neural Netw.*, vol. 16, no. 6, pp. 1477–1490, 2005.

[15] L. Jin, J. Yan, X. Du, X. Xiao, and D. Fu, "RNN for solving time-variant generalized Sylvester equation with applications to robots and acoustic source localization," *IEEE Trans. Ind. Inf.*, vol. 16, no. 10, pp. 6359–6369, 2020.

[16] L. Xiao, L. Li, P. Cao, and Y. He, "A fixed-time robust controller based on zeroing neural network for generalized projective synchronization of chaotic systems," *Chaos, Solitons Fractals*, vol. 169, p. 113279, 2023.

[17] Z. Fu, Y. Zhang, and N. Tan, "Gradient-feedback ZNN for unconstrained time-variant convex optimization and robot manipulator application," *IEEE Trans. Ind. Inf.*, 2023, in press with doi: 10.1109/TII.2023.3240737.

[18] L. Xiao, J. Dai, L. Jin, W. Li, S. Li, and J. Hou, "A noise-enduring and finite-time zeroing neural network for equality-constrained time-varying nonlinear optimization," *IEEE Trans. Syst., Man, Cybern., Syst.*, vol. 51, no. 8, pp. 4729–4740, 2019.

[19] D. Gerontitis, R. Behera, P. Tzekis, and P. Stanimirović, "A family of varying-parameter finite-time zeroing neural networks for solving time-varying Sylvester equation and its application," *J. Comput. Appl. Math.*, vol. 403, p. 113826, 2022.

[20] Z. Tan, L. Xiao, S. Chen, and X. Lv, "Noise-tolerant and finite-time convergent ZNN models for dynamic matrix Moore-Penrose inversion," *IEEE Trans. Ind. Inf.*, vol. 16, no. 3, pp. 1591–1601, 2019.

[21] B. Zhang, X. Lan, Y. Liu, G. Wang, and Z. Sun, "sEMG-based continuous motion estimation of upper limb using a novel noise-tolerant zeroing neurodynamic model combined with LSTM network," *Digital Signal Process.*, vol. 133, p. 103828, 2023.

[22] Z. Zhang, Z. Li, and S. Yang, "A barrier varying-parameter dynamic learning network for solving time-varying quadratic programming problems with multiple constraints," *IEEE Trans. Cybern.*, vol. 52, no. 9, pp. 8781–8792, 2022.

[23] X. Wang, Y. Sun, and D. Ding, "Adaptive dynamic programming for networked control systems under communication constraints: A survey of trends and techniques," *Int. J. Netw. Dyn. Intell.*, pp. 85–98, 2022.

[24] J. Cheng, Y. Wang, J. H. Park, J. Cao, and K. Shi, "Static output feedback quantized control for fuzzy Markovian switching singularly perturbed systems with deception attacks," *IEEE Trans. Fuzzy Syst.*, vol. 30, no. 4, pp. 1036–1047, 2021.

[25] Z. Ruan, Q. Yang, S. S. Ge, and Y. Sun, "Adaptive fuzzy fault tolerant control of uncertain MIMO nonlinear systems with output constraints and unknown control directions," *IEEE Trans. Fuzzy Syst.*, vol. 30, no. 5, pp. 1224–1238, 2022.

[26] V. N. Katsikis, P. S. Stanimirović, S. D. Mourtas, L. Xiao, D. Karabašević, and D. Stanujkić, "Zeroing neural network with fuzzy parameter for computing Pseudoinverse of arbitrary matrix," *IEEE Trans. Fuzzy Syst.*, vol. 30, no. 9, pp. 3426–3435, 2021.

[27] L. Jia, L. Xiao, and J. Dai, "Application of two fuzzy logic systems to complex-type ZNN models for the Drazin inverse of time-dependent complex-value matrix," *IEEE Trans. Fuzzy Syst.*, vol. 30, no. 9, pp. 3685–3694, 2021.

[28] J. Dai, L. Luo, L. Xiao, L. Jia, and X. Li, "An intelligent fuzzy robustness ZNN model with fixed-time convergence for time-variant Stein matrix equation," *Int. J. Intell. Syst.*, vol. 37, no. 12, pp. 11 670–11 691, 2022.

[29] J. Dai, X. Yang, L. Xiao, L. Jia, X. Liu, and Y. Wang, "Design and analysis of a self-adaptive zeroing neural network for solving time-varying quadratic programming," *IEEE Trans. Neural Netw. Learn. Syst.*, 2022, in press with doi: 10.1109/TNNLS.2021.3138900.

[30] H. Du and N. Zhang, "Application of evolving Takagi-Sugeno fuzzy model to nonlinear system identification," *Appl. Soft Comput.*, vol. 8, no. 1, pp. 676–686, 2008.

[31] Y. Shen, P. Miao, Y. Huang, and Y. Shen, "Finite-time stability and its application for solving time-varying Sylvester equation by recurrent neural network," *Neural Process. Lett.*, vol. 42, pp. 763–784, 2015.

[32] Y. Shen and Y. Huang, "Global finite-time stabilisation for a class of nonlinear systems," *Int. J. Syst. Sci.*, vol. 43, no. 1, pp. 73–78, 2012.

[33] C. Peng, J. Zhang, and Q. L. Han, "Consensus of multiagent systems with nonlinear dynamics using an integrated sampled-data-based event-triggered communication scheme," *IEEE Trans. Syst., Man, Cybern., Syst.*, vol. 49, no. 3, pp. 589–599, 2019.

[34] X. Huang and J. Dong, "Reliable leader-to-follower formation control of multiagent systems under communication quantization and attacks," *IEEE Trans. Syst., Man, Cybern., Syst.*, vol. 50, no. 1, pp. 89–99, 2020.

[35] Z. Li, Z. Duan, G. Chen, and L. Huang, "Consensus of multiagent systems and synchronization of complex networks: A unified viewpoint," *IEEE Trans. Circuits Syst. I, Reg. Papers*, vol. 57, no. 1, pp. 213–224, 2010.

[36] J. Dai, Y. Cao, L. Xiao, H. Tan, and L. Jia, "Design and analysis of a noise-suppression zeroing neural network approach for robust synchronization of chaotic systems," *Neurocomputing*, vol. 426, pp. 299–308, 2021.